Check for updates

RESEARCH ARTICLE

REVISED Numerical model of a top-blown rotary converter preheating and charge heating with an oxy-fuel burner

[version 2; peer review: 3 approved, 1 not approved]

Sergey Semenov[1], Patrick Namy[1], Aditya Kale[2], Sello Tsebe[2]

[1]SIMTEC, Grenoble, 38000, France
[2]MINTEK, Randburg, 2194, South Africa

v2 **First published:** 08 Nov 2024, **4**:248
https://doi.org/10.12688/openreseurope.18594.1
Latest published: 04 Jul 2025, **4**:248
https://doi.org/10.12688/openreseurope.18594.2

Abstract

Background

The present work is conducted in the framework of the SisAl Pilot EU project, which aims to optimize silicon production in Europe by recycling materials and using carbon-emission-friendly technology. Silicon production experiments were conducted on laboratory and pilot scales in different types of furnaces, including top-blown rotary converters (TBRC) used as chemical reactors for molten slag-metal mixtures. In addition to experimental work, process optimization also relies on numerical modelling.

Methods

In this study, COMSOL Multiphysics® was used for the numerical testing of a new thermal design of TBRC by simulating its preheating and charge heating owing to an external heat source provided by an oxy-fuel burner.

Results and conclusions

The risk of slag solidification in TBRC during the aluminothermic reduction of silica was assessed. The model predicts that, with a useful burner power of 600 kW, the empty TBRC can be preheated to 1650°C in less than 30 min. Based on this model, the optimum burner power for maintaining the TBRC charge in a liquid state was determined. The influence of the TBRC inclination angle and its rotation frequency was studied numerically.

Open Peer Review

Approval Status ✓ ✓ ✗ ✓

	1	2	3	4
version 2 (revision) 04 Jul 2025	✓ view	✓ view		✓ view
version 1 08 Nov 2024	? view	? view	✗ view	

1. **Neeraj Kumar Bhoi**, Banasthali University (Ringgold ID: 29803), Jaipur, India
2. **Laura Donato**, Universite Libre de Bruxelles, Brussels, Belgium
3. **Shibo Kuang**, Monash University, Clayton, Australia
4. **Theresa Coetsee**, University of Pretoria, Pretoria, South Africa

Any reports and responses or comments on the article can be found at the end of the article.

Keywords
Top-Blown Rotary Converter, Furnace Preheating, Charge Heating, Aluminothermic Reduction, Finite Element Method, COMSOL Multiphysics, Heat Transfer Modelling, Phase Change



This article is included in the Horizon 2020 gateway.

Corresponding author: Sergey Semenov (sergey.semenov@simtecsolution.fr)

Author roles: Semenov S: Writing – Original Draft Preparation; **Namy P**: Writing – Review & Editing; **Kale A**: Conceptualization; **Tsebe S**: Conceptualization

Competing interests: No competing interests were disclosed.

Grant information: This project has received funding from the European Union's Horizon 2020 research and innovation programme under grant agreement No 869268 (project name SisAl Pilot).

Copyright: © 2025 Semenov S *et al*. This is an open access article distributed under the terms of the Creative Commons Attribution License, which permits unrestricted use, distribution, and reproduction in any medium, provided the original work is properly cited.

How to cite this article: Semenov S, Namy P, Kale A and Tsebe S. **Numerical model of a top-blown rotary converter preheating and charge heating with an oxy-fuel burner [version 2; peer review: 3 approved, 1 not approved]** Open Research Europe 2025, **4**:248 https://doi.org/10.12688/openreseurope.18594.2

First published: 08 Nov 2024, **4**:248 https://doi.org/10.12688/openreseurope.18594.1

REVISED **Amendments from Version 1**

The revised research article differs from its previous version through an improved literature review and a series of clarifications in response to reviewers' feedback.

The position of present study within the broader context of the field is clarified. It is stressed that our focus was on addressing a specific engineering challenge within the SisAl Pilot project, rather than providing a comprehensive review of the field. The study contributes practical insights toward design verification rather than theoretical advancement.

The Introduction now presents chemical reactions of the traditional carbothermic reduction of silica and the aluminothermic reduction proposed by the SisAl Pilot project and discusses the advantages of the new approach. It also includes more thorough literature analysis regarding the numerical modelling of rotary furnaces, as well as the sustainability and economic viability of the SisAl process.

In the "Governing equations", the simplifying hypotheses are discussed regarding modelling interfaces among gas, metal and slag. The coupling between heat transfer and fluid flow equations, as well as between phases, is clarified throughout the section. The phase change modelling approach is explicitly described at the beginning of Section 4.3.

In Section 6.3, the supposed 20 min duration of aluminothermic reaction is justified by earlier published experimental measurements. Figure 4, Figure 7, Figure 8, Figure 12, Figure 13 and Figure 15 are revised to improve the clarity and to facilitate their interpretation. Overall numerical findings and general takeaways are summarized at the end of Section 6 and in Conclusions.

Any further responses from the reviewers can be found at the end of the article

1. Introduction

This work was conducted in the framework of the SisAl Pilot EU project, which is focused on demonstrating the possibility of metallurgical-grade silicon production at the pilot scale based on the aluminothermic reduction of silica. The traditional carbothermic reduction of silica[1–3] in a submerged arc furnace (SAF) involves multiple chemical reactions in all phases (solid, liquid and gaseous). In an idealized form, the overall reduction process can be represented by the following chemical reaction[1,3]:

$$SiO_2 + 2\,C \rightleftharpoons Si + 2\,CO$$

In comparison with the traditional carbothermic reduction of silica[1–3], the advantage of the proposed aluminothermic reduction technology is its low CO2 emissions and the possibility to recycle generated waste back into the process[4]. Additionally, the exothermic nature of the aluminothermic reaction provides energy efficiency and lowers the required temperature[4]. The main chemical reaction involved is shown below[4]:

$$4\,Al + 3\,SiO_2\ (\text{in CaO-}SiO_2\ \text{slag}) \rightleftharpoons 3\,Si + 2\,Al_2O_3\ (\text{in CaO-}Al_2O_3\ \text{slag})$$

A preliminary economic assessment of the SisAl process is considered in 5. Unlike the gas-solid reactions in the conventional carbothermic process, the SisAl process operates through liquid-liquid reactions. This eliminates the need for specific mechanical strength and particle size requirements for the quartz material. As a result, the SisAl process can utilize less commonly used and more cost-effective silica (SiO_2) sources[5]. Relatively expensive quicklime (CaO) can also be replaced by cheaper secondary materials from the mining or metallurgical industries[5]. Aluminum is the most expensive raw material in the SisAl process, making white dross a cost-effective alternative for pilot testing[5].

As part of the SisAl Pilot project, the numerical modelling support of the experimental works was stipulated. One of these efforts is focused on developing a numerical model of a top-blown rotary converter (TBRC) heated by an oxy-fuel burner. Within the SisAl Pilot project, this metallurgical reactor for the aluminothermic reduction of silica was proposed by MINTEK as an alternative to an electric furnace to mitigate the risks associated with the interruption of the electrical power supply due to load shedding in South Africa. This type of reactor offers operational flexibility, enhanced mixing behavior, and potential for continuous processing. Unlike traditional converters or rotary kilns, the TBRC enables better control over temperature and chemical reactions through its unique combination of rotary motion and top-blown gas or flame injection.

Several literature sources report the results of numerical modelling of heat and mass transfer in rotary furnaces. Examples of numerical models of heat transfer in a rotary furnace heated by gas burners in the presence of charge can be found in 6 and 7. Gas flow models are reported in 8 and 9. A multiphase computational fluid dynamics model of charge stirring with oxygen jets and argon injection is presented in 10. Recent numerical work on a rotary furnace[11] models its preheating with a gas burner, as well as heat transfer and charge flow

during furnace operation. Most existing literature focuses either on empirical or post-operational data. Limited work has been published on predictive numerical modeling to validate TBRC design performance prior to construction, especially within project-specific constraints like those of the SisAl Pilot project. This study addresses this research gap by conducting a numerical investigation aimed at validating a specific TBRC design before physical construction.

Key distinguishing aspects of our work compared to previous studies of rotary converters were the geometry of the problem, the refractory materials and the operating conditions, which directly influence the flow dynamics and heat transfer in TBRC. The objective of the present modelling work was to test the thermal performance of TBRC during the preheating and aluminothermic reduction stages. Molten slag (50wt%CaO-50wt%SiO_2) and aluminum are planned to be prepared in separate furnaces outside the TBRC and then poured into the TBRC for aluminothermic reduction to take place. The risk of slag solidification in TBRC during the aluminothermic reduction stage needs to be assessed. The optimal burner power for maintaining the TBRC charge in the liquid state must be determined. The influence of the TBRC inclination angle and its rotation frequency should also be numerically studied. By aligning the modeling approach with the functional needs of the SisAl Pilot project, the study contributes practical insights toward design verification rather than theoretical advancement. In Section 2 and Section 3, the model geometry and numerical methods are described, respectively. Section 4 and Section 5 present the governing equations and material properties, respectively. In Section 6, numerical results are presented and discussed. Finally, Section 7 concludes the paper.

2. Problem geometry

The geometry and dimensions of the top-blown rotary converter (TBRC) were based on technical drawings provided by MINTEK. The corresponding numerically modelled axisymmetric geometry of the TBRC and materials are shown in Figure 1. The steel shell is not modelled because its geometry is not known prior to furnace construction, and because its contribution to the wall's thermal resistance is insignificant owing to the high thermal conductivity of steel and the relatively small shell thickness. The heights H_s and H_m of the slag and metal layers inside the TBRC are modelled based on the materials' initial volumes $V_{0,s}$ and $V_{0,m}$ and on the geometry of internal cavity of the TBRC, which depends on its spatial orientation.

Two TBRC orientations were numerically modelled in this work: vertical orientation (see Figure 2 (a)) and hypothetical horizontal orientation (see Figure 2 (b)). The initial volumes $V_{0,s}$ and $V_{0,m}$ of slag and metal, respectively, are computed from their initial masses $m_{0,s}$ = 500 kg and $m_{0,m}$ = 150 kg and their initial densities $\rho_{0,s}(T_{0,s}, \mathbf{X}_{0,s})$ and $\rho_{0,m}(T_{0,m}, \mathbf{X}_{0,m})$ which depend on their initial temperatures $T_{0,s}$ and $T_{0,m}$ and initial compositions $\mathbf{X}_{0,s}$ and $\mathbf{X}_{0,m}$.

$$V_{0,k} = m_{0,k}/\rho_{0,k}(T_{0,k}, \mathbf{X}_{0,k}), \qquad k = s, m$$

$$\mathbf{X}_{0,S} = (X_{0,SiO_2}, X_{0,Al_2O_3}, X_{0,CaO})$$

$$\mathbf{X}_{0,m} = (X_{0,Si}, X_{0,Al}, X_{0,Ca})$$

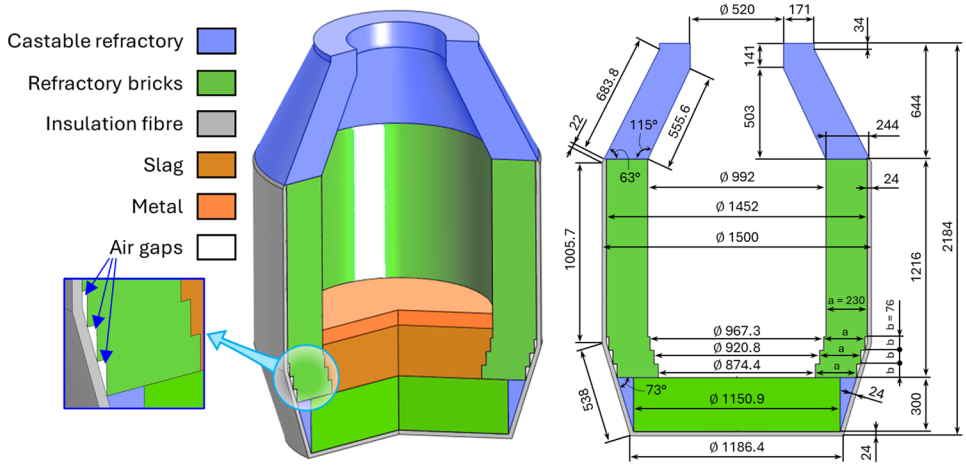

Figure 1. Modelled axisymmetric geometry of TBRC. Dimensions in mm.

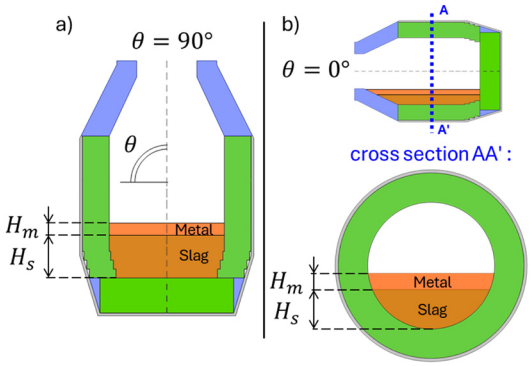

Figure 2. Numerically modelled orientations of TBRC. (**a**): Vertical orientation. (**b**): Horizontal orientation.

where the subscripts s and m stand for slag and metal, respectively, $X_{0,i}$ stands for the initial mole fraction of species i.

3. Methods

This problem was solved using the finite element software COMSOL Multiphysics® version 6.1 (www.comsol.com, a copyright license is obtained). Modules of Heat Transfer, Turbulent Flow k–ω, and Surface-to-Surface Radiation were used to set up the model physics. The temperature and velocity fields were spatially discretized using quadratic elements, whereas the pressure and surface radiosity were discretized using linear elements. Time integration is performed with a Backward Differentiation Formula (BDF) of orders 1 to 2. The computational domain was spatially discretized with a triangular mesh which consists of 27 600 finite elements (see Figure 3), resulting in 220 700 degrees of freedom. The computations were performed on two laptops with eight physical cores, an Intel processor with 64 GB RAM, and a workstation with 64 physical cores and 1 TB RAM.

4. Governing equations

The physics of the problem includes heat transfer in solids and fluids with phase change, surface-to-surface radiation, and a turbulent k–ω model to simulate slag and metal flow. All the transport equations and boundary conditions were similar for both the vertical and horizontal orientations of the TBRC. Without a loss of generality, only the vertical configuration is presented in this section.

4.1. Fluid dynamics in metal phase

Unsteady incompressible RANS equations with k-ω turbulence model are solved in the metal domain:

$$\rho(\partial\mathbf{u}/\partial t+\mathbf{u}\cdot\nabla\mathbf{u})=\nabla\cdot[-p\mathbf{I}+\mathbf{K}]+\rho\mathbf{g}$$

$$\nabla\cdot\mathbf{u}=0$$

$$\rho(\partial k/\partial t+\mathbf{u}\cdot\nabla k)=\nabla\cdot[\mu_k\nabla k]+P_k-\beta_0^*\rho\omega k$$

$$\rho\left(\frac{\partial\omega}{\partial t}+\mathbf{u}\cdot\nabla\omega\right)=\nabla\cdot[\mu_\omega\nabla\omega]+\alpha\frac{\omega}{k}P_k-\beta_0\rho\omega^2$$

$$\mathbf{K}=(\mu+\mu_T)(\nabla\mathbf{u}+(\nabla\mathbf{u})^\top),\quad \mu_T=\rho k/\omega,\quad \mu_k=\mu+\mu_T\sigma_k^*,\quad \mu_\omega=\mu+\mu_T\sigma_\omega$$

$$P_k=\mu_T\left[\nabla\mathbf{u}:\left(\nabla\mathbf{u}+(\nabla\mathbf{u})^\top\right)\right],\quad \alpha=0.52,\quad \sigma_k^*=0.5,\quad \sigma_\omega=0.5,\quad \beta_0=0.072,\quad \beta_0^*=0.09$$

In this model, the turbulent viscosity μ_T was calculated from two additional fields: the turbulent kinetic energy k and the specific rate of dissipation of the turbulent kinetic energy ω. The axial symmetry condition was applied at $r=0$:

$$u_r=0,\quad \partial\zeta/\partial r=0,\quad \text{where } \zeta=u_r,u_z,p,k,\omega$$

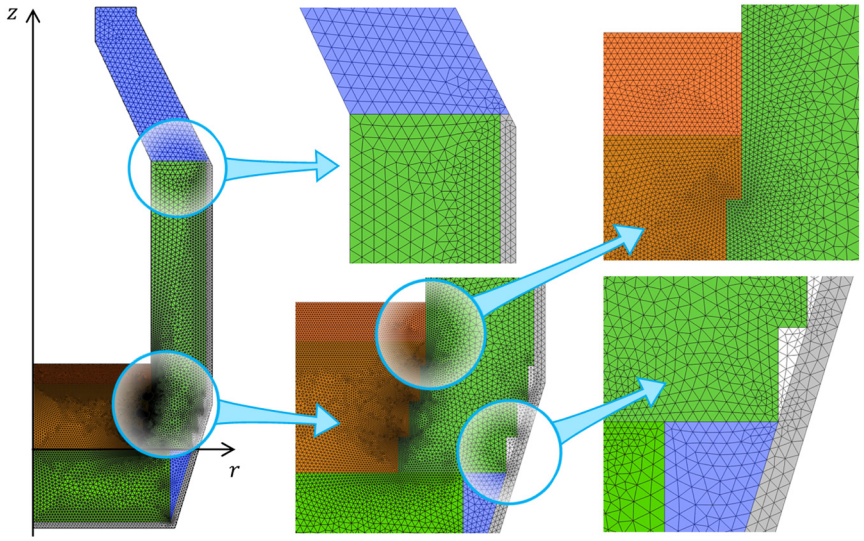

Figure 3. Computational mesh.

The interfaces among gas, metal and slag are assumed to be fixed in space. The free surface displacement is disregarded, since the stratification of the phases in the Earth's gravitational field is assumed to prevent significant interfaces displacement. Slip boundary condition is imposed on the upper metal surface justified by the fact that air above the metal has significantly lower viscosity and exerts negligible stress on the metal surface:

$$\mathbf{u}\cdot\mathbf{n}=0,\quad \mathbf{K}_{\mathbf{n}}-(\mathbf{K}_{\mathbf{n}}\cdot\mathbf{n})\mathbf{n}=0,\quad \mathbf{K}_{\mathbf{n}}=\mathbf{K}\cdot\mathbf{n}$$

$$\nabla k\cdot\mathbf{n}=0,\quad \nabla\omega\cdot\mathbf{n}=0$$

A no-slip condition is imposed on the metal-slag (MS) and metal–refractory (MR) interfaces to ensure tangential momentum transfer between the phases. The metal moves tangentially to the interface with the velocity of slag $\mathbf{u}_s$ at the MS interface or with the velocity of the rotating refractory $\mathbf{u}_{rot}$ at the MR interface owing to TBRC rotation about its axis of symmetry:

$$\mathbf{u}\cdot\mathbf{n}=0,\quad \mathbf{K}\cdot\mathbf{n}=-\rho u^{*}u_{\tau}\mathbf{u}_{\tau}/|\mathbf{u}_{\tau}|,\quad \nabla k\cdot\mathbf{n}=0$$

$$\omega=(\omega_{visc}^{2}+\omega_{log}^{2})^{1/2},\quad \omega_{visc}=6\mu/(\rho\beta_0\delta_w^{2}),\quad \omega_{log}=u^{*}/\left(\kappa_{\mathrm{v}}\delta_w\sqrt{\beta_0^{*}}\right)$$

$$\mathbf{u}_{\tau}=\mathbf{n}_{rel}-(\mathbf{u}_{rel}\cdot\mathbf{n})\mathbf{n},\quad \mathbf{u}_{rel}=\mathbf{u}-\mathbf{u}_{bnd},\quad \mathbf{u}_{bnd}=\begin{cases}\mathbf{u}_s, & \text{at MS interface}\\ \mathbf{u}_{rot}, & \text{at MR interface}\end{cases}$$

$$u_{rot,r}=0,\quad u_{rot,\varphi}=r\omega_{rot},\quad u_{rot,z}=0,\quad u^{*}=\left[u_{\tau,visc}^{4}+(u_{log}^{*})^{4}\right]^{\frac{1}{4}},\quad u_{\tau}=\left[u_{\tau,visc}^{4}+u_{\tau,log}^{4}\right]^{\frac{1}{4}}$$

$$u_{log}^{*}=\sqrt{\max(0,k)\sqrt{\beta_0^{*}}},\quad u_{\tau,visc}=\sqrt{\mu|\mathbf{u}_{\tau}|/(\rho\delta_w)},\quad u_{\tau,log}=|\mathbf{u}_{\tau}|\kappa_{\mathrm{v}}/(\ln[\max(1,\delta_w^{+})]+B\kappa_{\mathrm{v}})$$

$$\delta_w^{+}=\rho u^{*}\delta_w/\mu,\quad \kappa_{\mathrm{v}}=0.41,\quad \mathrm{B}=5.2$$

where $\mathbf{n}$ is the unit normal vector at the interface, ω_{rot} is the angular velocity of the TBRC rotation, and δ_w is the wall lift-off distance, which equals half of the size of the near-wall element. Ambient pressure p_{amb} was imposed at the right top corner of the metal domain.

The above no-slip boundary condition at the metal-slag interface together with the condition of tangential stress continuity (see the next subsection) result in a bi-directional coupling of fluid flow equations of slag and

metal at the interface. The temperature dependence of material properties, such as density and viscosity, as well as heat advection and turbulent thermal conductivity result in a bi-directional coupling of flow and heat transfer equations.

4.2. Fluid dynamics in slag phase

Similar unsteady incompressible RANS equations with k–ω turbulence model were solved in the slag domain. The only difference is that in the solid or porous phase of the slag, the Darcy force $\mathbf{f}_D$ is added as follows:

$$\mathbf{f}_D = -\mu(\mathbf{u} - \mathbf{u}_{rot})/K_{perm}$$

where μ is the intrinsic slag viscosity, and K_{perm} is the slag permeability (Kozeny-Carman model).

$$K_{perm} = K_0 g_l^3/(1-g_l)^2$$

where $K_0 = 7 \times 10^{-9}$ m^2 and g_l is the liquid fraction. Additional source terms related to the Darcy force were also added to the right-hand side of the turbulence equations[12]: $-2\mu k/K_{perm}$ in the k equation and $-2\mu\omega/K_{perm}$ in the ω equation. The boundary condition of tangential stress continuity and zero normal velocity was applied at the slag-metal interface as follows:

$$\boldsymbol{\sigma}_{\tau,slag} = \boldsymbol{\sigma}_{\tau,metal}, \quad \boldsymbol{\sigma}_\tau = \boldsymbol{\sigma} - (\boldsymbol{\sigma}\cdot\mathbf{n})\mathbf{n}$$

$$\boldsymbol{\sigma} = [-p\mathbf{I} + \mathbf{K}]\cdot\mathbf{n} \text{ (same } \mathbf{n} \text{ for both the slag and metal)}$$

$$\mathbf{u}\cdot\mathbf{n} = 0, \quad \nabla k\cdot\mathbf{n} = 0,\ \nabla\omega\cdot\mathbf{n} = 0$$

The use of this boundary condition is justified by the fact that slag moves owing to the shear stress of the tangential metal flow above it, while the interface displacement in the normal direction is neglected. Together with the no-slip boundary condition provided in the previous subsection, the above boundary conditions establish a closed and solvable system of equations at the metal-slag interface, also resulting in a bi-directional coupling of flow equations in slag and metal. The no-slip condition at the slag-refractory interface and the axial symmetry condition at $r = 0$ are imposed with equations similar to those in the previous subsection. The hydrostatic pressure of the metal layer was applied at the top-right corner of the slag domain. As stated in the previous subsection, the flow and heat transfer equations are bi-directionally coupled due to temperature-dependent properties of materials, such as density and viscosity.

4.3. Heat transfer with surface-to-surface radiation

We use the Apparent Heat Capacity method to model slag solidification. According to the method, the enthalpy of fusion is smoothly redistributed in a particular range of temperatures around the melting point and is included in the specific heat capacity at constant pressure c_p, resulting in a modified heat capacity c_p'. In other materials, where phase change does not occur, the modified heat capacity c_p' coincides with c_p. Thus, the following heat equation is solved in all domains:

$$\rho c_p'(\partial T/\partial t + \mathbf{u}\cdot\nabla T) + \nabla\cdot\mathbf{q} = 0$$

$$\mathbf{q} = -(k + k_T)\nabla T$$

where T is the temperature, ρ is the density, $\mathbf{u}$ is the velocity, $\mathbf{q}$ is the conductive heat flux, k and k_T are the molecular and turbulent thermal conductivity, respectively.

$$k_T = c_p\mu_T/\mathrm{Pr}_T$$

where μ_T is the turbulent viscosity and Pr_T is the turbulent Prandtl number, which is often modelled as a function of the molecular Prandtl number Pr[13]. For simplicity, a constant value of the turbulent Prandtl number was adopted in this numerical study:

$$\mathrm{Pr}_T = 0.85$$

The heat transfer is strongly coupled with the fluid flow. Convective heat transfer is driven by the fluid motion, with velocity fields influencing temperature distribution. Additionally, the turbulence model accounts for enhanced thermal transport by incorporating turbulent thermal conductivity, which plays a key role in energy

exchange within the system. On the other hand, the temperature dependence of material density and viscosity implies the influence of heat transfer on the fluid flow.

In the solid domains, the convective term ($\mathbf{u} \cdot \nabla T$) and turbulent conductivity k_T are omitted. In the solid phase of the slag layer, these terms are suppressed with the help of the Darcy force (see Subsection 4.2). The condition of axial symmetry at $r = 0$ is

$$\partial T / \partial r = 0$$

Temperature is continuous on all material interfaces:

$$T_{up} = T_{down}$$

where subscripts *up* and *down* denote the upward and downward sides of the interface, respectively, *up* corresponds to the material to which the unit normal vector $\mathbf{n}$ is pointing. The condition of the heat flux continuity/discontinuity at the material interfaces is

$$\mathbf{q}_{up} \cdot \mathbf{n} - \mathbf{q}_{down} \cdot \mathbf{n} = q$$

where q denotes the surface density of the interfacial heat source. In contrast to reference 11, where gas temperature is used as a boundary condition, in the present work the useful burner power is imposed on internal boundaries of the rotary converter. This helps to avoid artificial energy production on internal surfaces of the converter and ensures global energy conservation. Thus, the boundary heat source provided by an oxy-fuel burner on the internal surfaces of the TBRC is

$$-\mathbf{q} \cdot \mathbf{n} = q_{burner}$$

where the unit normal vector $\mathbf{n}$ at the metal-air or refractory-air interface points into the air. Interfacial heat source due to the exothermic aluminothermic reaction at the metal-slag interface

$$-[\mathbf{q}_{slag} - \mathbf{q}_{metal}] \cdot \mathbf{n}_{slag} = q_{reaction}$$

where $\mathbf{n}_{slag}$ is pointing to the metal and $q_{reaction}$ is the surface density of the reaction power computed from the reaction enthalpy and reaction time. The heat flux due to external natural convection is applied to the external TBRC boundaries as follows:

$$-\mathbf{q} \cdot \mathbf{n} = h(T_{amb} - T)$$

where $\mathbf{n}$ is the outward unit normal vector and h is the heat transfer coefficient, computed according to the empirical models of external natural convection. On the interfaces and boundaries that participate in the surface-to-surface radiation (all external and internal surfaces of TBRC, as well as interfaces of air gaps), an additional boundary heat source q_r is imposed owing to thermal radiation absorption:

$$q_r = \varepsilon(G - \sigma_{SB} T^4)$$

where ε is the hemispherical emissivity of the radiating surface, σ_{SB} is the Stefan-Boltzmann constant, and G is the surface irradiance.

5. Material properties and parameters

5.1. Refractory materials and air

The thermal properties of all refractory materials were provided by MINTEK[14]: VR 90B alumina-silicate was used for the refractory bricks (see Table 1), L-Cast 18 alumina-silicate for the castable refractory (see Table 2), and 1260 ST-RB ceramic fiber blankets for the insulation fiber (see Table 3).

The specific heat capacity at constant pressure $c_p(T)$ is approximated based on materials composition:

$$c_p(T) = \sum_i \omega_i c_{p,i}(T), \quad i = \mathrm{SiO_2}, \mathrm{Al_2O_3}, \text{etc.}$$

where ω_i is the mass fraction and $c_{p,i}(T)$ is the specific heat capacity of component i from the NIST database[15]. The thermal conductivity $k(T)$ of the 1260 ST-RB ceramic fiber blanket was modelled as a function of temperature by linear interpolation between the given data points. A constant-value extrapolation of all properties

Table 1. Properties of VR 90B refractory bricks.

Parameter	Value
Thermal conductivity at 1000°C	1.4 W/m/K
Bulk density	2900 kg/m^3
Mass fraction of: SiO_2/ Al_2O_3/ Fe_2O_3/ TiO_2/ CaO/ MgO/ Na_2O/ K_2O	9/ 90/ 0.2/ 0.2/ 0.1/ 0.1/ 0.2/ 0.2 wt%

Table 2. Properties of L-Cast 18 castable refractory.

Parameter	Value
Thermal conductivity at 1000°C	2.8 W/m/K
Bulk density	2940 kg/m^3
Mass fraction of: SiO_2/ Al_2O_3/ Fe_2O_3/ TiO_2/ CaO/ MgO	5.1/ 92.2/ 0.1/ 0.8/ 0.9/ 0.9 wt%

Table 3. Properties of 1260 ST-RB ceramic fibre blanket.

Parameter	Value
Thermal conductivity at: 600/ 800/ 1000°C	0.15/ 0.22/ 0.30 W/m/K
Bulk density	128 kg/m^3
Mass fraction of SiO_2/ Al_2O_3	57/ 43 wt%

was used for out-of-range temperatures. The air gaps (see Figure 1) are assumed to be filled with air, and their properties are taken from the COMSOL Multiphysics® materials library.

5.2. Slag and metal

In the metal phase, initially pure Al becomes an Al-Si-Ca alloy as it reacts with the slag. Similarly, initially SiO_2-CaO slag becomes Al_2O_3-SiO_2-CaO slag as it reacts with the metal. Thus, the slag and metal densities are modelled as functions of the temperature T and composition X_i (mole fraction of component i):

$$\rho(T, X_i) = \sum_i [X_i M_i] \Big/ \left(\sum_i [X_i V_{mol,i}(T)] + V^{EX} \right)$$

where M_i and $V_{mol,i}$ are the molar mass and molar volume[16–19] of component i, V^{EX} is a corrective interaction term[19], i = Al, Si, Ca for metal, and i = Al_2O_3, SiO_2, CaO for slag. The composition of the slag and metal is modelled as a function of the relative reaction extent ξ_{rel} which equals 0 at the beginning of the process and 1 at the end of the reaction:

$$X_i = X_{i,init} + \xi_{rel} \left(X_{i,final} - X_{i,init} \right)$$

For simplicity, ξ_{rel} is a linear function of time:

$$\xi_{rel} = t/t_r$$

where t_r is the user-defined reaction time. The initial $X_{i,init}$ and final $X_{i,final}$ compositions, as well as the reaction energy, were estimated using the software provided by the project partner SINTEF. This artificial neural network-based tool[20,21] was trained on FactSage® data for the metal-slag system of interest. Other metal properties, such as thermal and electrical conductivity[16], dynamic viscosity[22], and heat capacity at constant pressure, were computed as for pure aluminum. The thermal conductivity of the slag was assumed to be constant and equal to 1 W/m/K. The slag viscosity was modelled as a function of the temperature and slag composition according to the mathematical model[21] of Kai Tang from SINTEF. Other slag properties, such as heat capacity, enthalpy, and electrical conductivity, were computed as functions of temperature and composition, according to the Ken Mills model[23].

6. Numerical results and discussion

6.1. TBRC preheating

The unsteady process of empty TBRC preheating with an oxy-fuel burner was numerically modelled, as shown in Figure 4. It was found that the surface of the refractory bricks (inside the TBRC) could reach the desired temperature of 1650°C in less than 30 min when the useful burner power was 600 kW, as shown in Figure 5. At the same time, the volume-averaged temperature of the bricks at t = 0.5 h stays below 200°C, meaning that the refractory volume remains relatively cold with respect to the internal TBRC surface. Further preheating resulted in a significant temperature increase, as shown in Figure 5, where the average temperature of the brick surface reached 2400°C after 12 h of preheating and 2454°C in the steady state (as $t \to \infty$). Fig. Figure 6 shows the power balance of the system. The only heat source in the furnace was the oxy-fuel burner with a constant input power of 600 kW (blue line and arrows in Figure 6). Power is lost by three principal mechanisms: external natural convection (green line and arrows in Figure 6), thermal radiation from the external surface of the TBRC (orange line and arrows in Figure 6), and thermal radiation from the inside of the TBRC through the opening at the top of the furnace (red line and arrows in Figure 6). Black square markers represent the difference between the input power and sum of the power losses. As can be seen in Figure 6 (right), a perfect power balance is numerically achieved for all simulated times: black square markers coincide with the rate of furnace heating (see magenta line in Figure 6), which is computed as follows:

$$\text{rate of furnace heating} = \int_V \rho c_p'(T) \frac{\partial T}{\partial t} dV$$

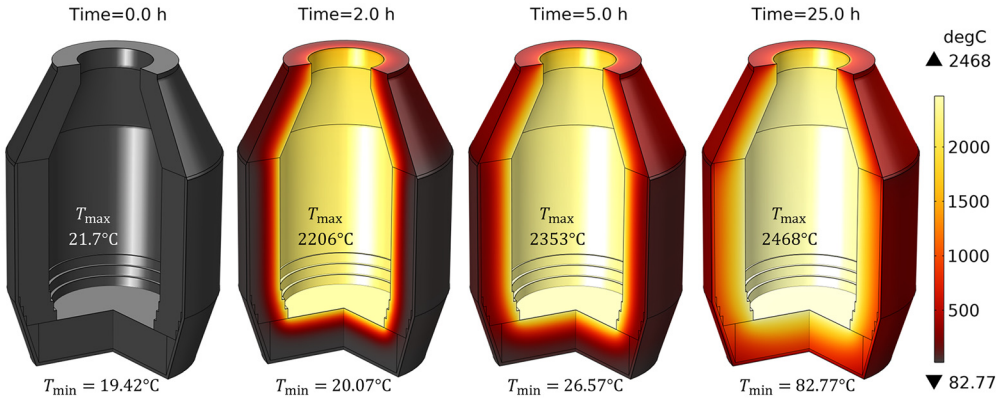

Figure 4. Time evolution of the temperature field at 600 kW burner power in an empty TBRC.

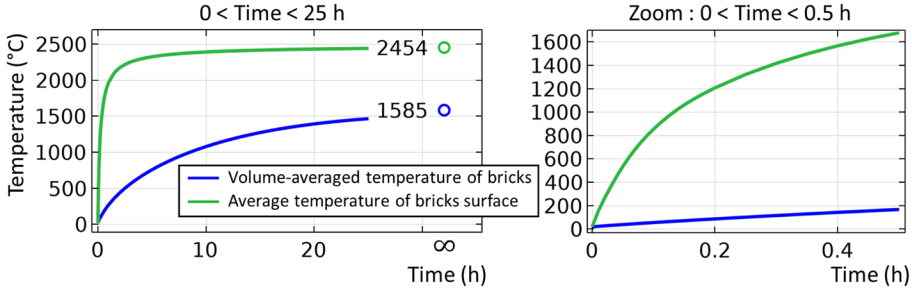

Figure 5. Average temperature of refractory bricks during 25 hours of preheating at 600 kW burner power.

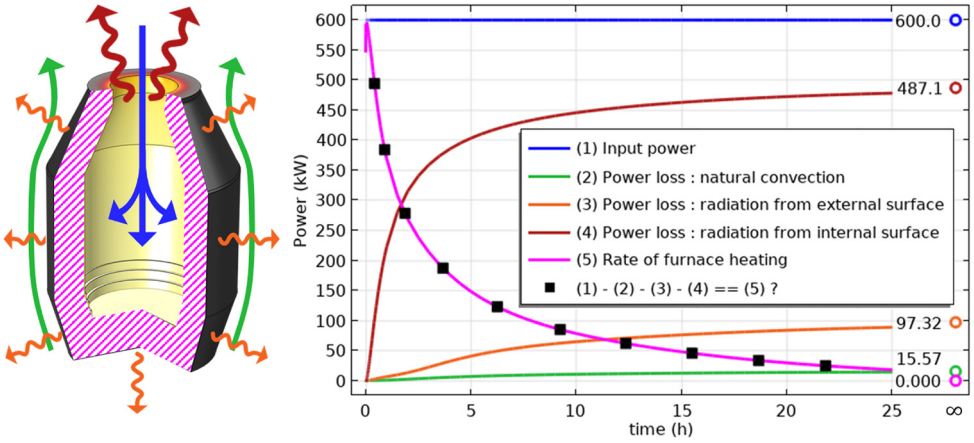

Figure 6. Left: heat fluxes contributing to the power balance. Right: time evolution of the power balance.

where integration is performed over the entire TBRC volume, V. At the beginning of preheating ($t = 0$), all types of power losses were small because the TBRC was still cold. Thus, at $t = 0$ the entire burner power (600 kW) was spent on furnace heating (magenta line in Figure 6). As the furnace body became hotter with time, the power losses increased. It was found that at steady state ($t \to \infty$), most of the power (81.2%) was lost in the form of thermal radiation from the internal surface of the TBRC towards the ambient environment through the opening at the top of the furnace. Therefore, the use of a furnace lid is recommended to prevent significant heat loss during operations that do not involve charging, tapping, or heating with a burner. The TBRC state after 30 min of preheating with 600 kW input power (see Figure 7) served as the initial condition for further computations with a furnace charge.

6.2. Influence of TBRC rotation frequency

Let us consider TBRC charged with only slag that rotates in its horizontal position ($\theta = 0$, see Figure 2). This configuration of the furnace was simulated using a 2D plane model that represents the TBRC cross-section, as shown in Figure 2 (b). The initial slag temperature was 1670°C. The initial temperature field in the TBRC refractory and air above the slag were taken from the previously solved preheating problem, as shown in Figure 7 (right). The dominant heat transfer mechanism in the air phase was surface-to-surface radiation. Therefore, to simplify the problem, air convection was not solved, and only air conduction was considered. The TBRC rotation frequency is initially zero (0 rpm at $t = 0$) and then smoothly increases to a given value during the first 10 s of the simulated process. The temperature field and slag velocity for a full burner power (600 kW) and a rotation frequency of 5 rpm are shown in Figure 8. The maximum temperature is located on the slag surface exposed to burner heating, while its minimum is always on the external surface of the TBRC refractory. The corresponding time evolution of slag temperature is shown in Figure 9. The minimum and maximum temperatures are indicated by the blue and red lines, respectively.

For $t < 20$ s, the flow is not yet fully established in the entire slag volume owing to the recent activation of TBRC rotation. This resulted in poor slag stirring during the first 20 s and, consequently, poor thermal conductivity of the slag layer. Thus, its maximum temperature T_{max} quickly rises to 1860°C on the surface heated by the burner, and its minimum temperature T_{min} quickly reduces to 1630°C at the bottom of the slag layer owing to heat losses to the ambient environment through the refractory. At $t = 20$ s, when the slag flow was fully established in the entire slag volume, more intensive stirring resulted in a decrease of T_{max} down to 1810°C and an increase of T_{min} up to 1650°C. Between 50 and 200 s, the maximum slag temperature slowly increases on its surface because of burner heating, whereas its minimum temperature remains almost constant and equal to the initial slag temperature $T_{0,s}$ = 1670°C. This minimum is found in the middle of the flow vortex, where the velocity is low and heat transfer occurs primarily through conduction. Thus, the low intrinsic thermal conductivity of the slag results in very slow temperature changes in the middle of the flow vortex. At 200 s, there was a qualitative change in the temperature behavior: the difference between T_{max} and T_{min} suddenly decreased. This can be explained by the spontaneous transition to a turbulent flow regime. Indeed, the turbulent slag viscosity μ_T is zero for $t < 200$ s, whereas the intrinsic viscosity (≈0.123 Pa·s) dominates, which corresponds to a laminar flow regime. However, after 200 s, the turbulent viscosity (≈1 Pa·s) dominated the intrinsic viscosity (≈0.117 Pa·s), as shown in Figure 10, which corresponds to a turbulent flow regime.

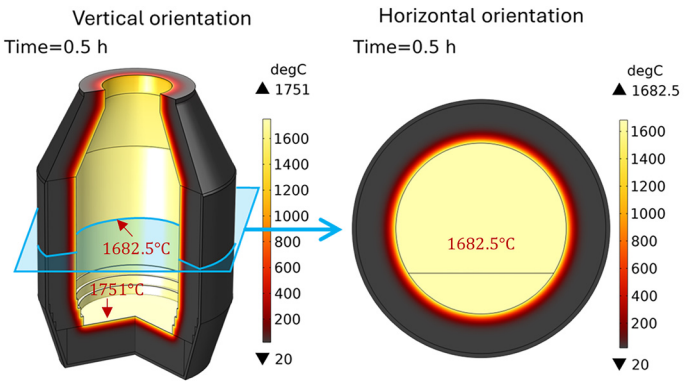

Figure 7. **TBRC after 30 min of preheating with 600 kW burner power, initial condition for further computations.**

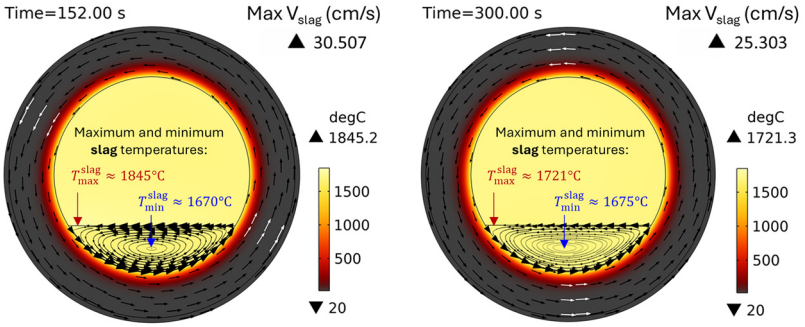

Figure 8. **Temperature field and slag velocity at 5 rpm and 600 kW burner power in a horizontal TBRC.**

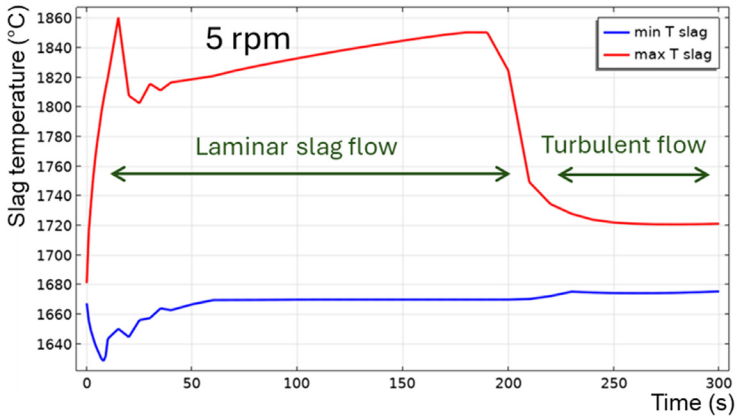

Figure 9. **Maximum and minimum slag temperature at 5 rpm and 600 kW burner power in a horizontal TBRC.**

In general, turbulence intensifies the heat transfer in the bulk of the fluid owing to turbulent mixing at multiple length scales. In the present numerical model, this effect causes a reduction in the temperature difference between T_{max} and T_{min} in the slag layer for $t > 200$ s. Qualitatively, the transition to a turbulent flow regime can be explained using the Reynolds number:

$$\mathrm{Re} = \rho u L / \mu = \rho R_{int} \omega_{rot} H_s / \mu$$

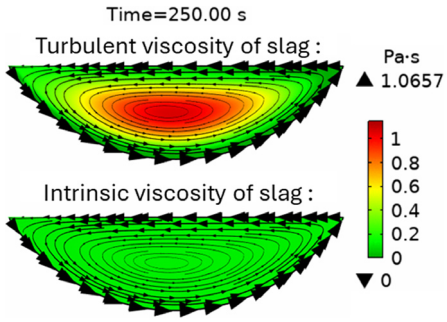

Figure 10. Intrinsic and turbulent slag viscosity at t = 250 s at 5 rpm and 600 kW burner power in a horizontal TBRC.

where ρ is the slag density, L is the characteristic length of the problem (height of the slag layer in this case $L = H_s$), $u = R_{int}\omega_{rot}$ is the flow velocity, R_{int} is the internal radius of the TBRC, and $\omega_{rot} = 2\pi \cdot 5$ rpm = 0.52 rad/s is the angular velocity of the TBRC rotation. As the slag is continuously heated by the burner, its average temperature increases, resulting in a reduction in its average intrinsic viscosity μ. This leads to a continuous increase in the Reynolds number, as shown in Figure 11, until it reaches a threshold value (1340 in this case) that triggers turbulence. The exact threshold value can be a complicated function of problem parameters and geometry.

The transition to a turbulent flow regime occurs spontaneously, similar to an avalanche (see T_{max} at t = 200 s in Figure 9), because of the positive feedback loop: the intensification of turbulence results in the intensification of heat transfer, which increases the average slag temperature and reduces its average intrinsic viscosity, which further intensifies the turbulence. When TBRC rotates faster, the Reynolds number increases; therefore, the spontaneous transition to a turbulent flow regime occurs earlier (see the 5–20 rpm cases in Figure 12). When the TBRC does not rotate, only natural convection due to buoyancy forces in Earth's gravity is present in the slag layer. In this case, the slag velocity was much lower than that in the forced-convection case. Thus, poor slag mixing results in a significant temperature difference across the layer (see the 0 rpm case in Figure 12) and slag freezing at the bottom of the pool (see the dashed line in Figure 12 representing the slag solidification temperature). Let us now consider the influence of the rotation frequency in vertically oriented TBRC (θ = 90°) (see Figure 2 (a)). The temperature and velocity fields are shown in Figure 13 for a rotation frequency of 10 rpm at t = 10 and 900 s (note that the total simulated duration was 1800 s). Slag velocity in the $r\varphi$ plane reaches 52 cm/s due to furnace rotation, whereas in the rz plane it remains below 0.18 cm/s for $t \geq 900$ s. This is explained by the fact that, in vertical TBRC, slag rotates together with TBRC about its axis of symmetry, whereas its vertical position is not perturbed by rotation. In contrast, in horizontally oriented TBRC, as shown in Figure 8, when the furnace rotates, it drags slag up against the gravity force, which in turn brings it down to the original level and therefore induces stirring. Thus, in vertical TBRC, any rotation frequency is insufficient for slag stirring, resulting in a significant temperature difference across the slag layer (see Figure 14). As a result, slag freezing occurs at the bottom of the pool (see the dashed line in Figure 14 representing the slag solidification temperature and liquid fraction isolines in Figure 13). The above results show that a vertical TBRC orientation is most unfavorable for slag stirring and leads to its solidification, whereas a horizontal TBRC orientation is the most favorable for stirring and works well as long as the furnace rotates, even at 1 rpm.

6.3. Influence of the burner power and of TBRC inclination angle

In this subsection, a TBRC charged with slag and metal is numerically modelled, considering an additional heat source at the metal-slag interface owing to aluminothermic reduction. Experimental investigations[24], carried out in the framework of the SisAl Pilot project, have indicated that the oxygen flux across the metal-slag interface, associated with the aluminothermic reaction, drops significantly after first 20 minutes of the reduction process. More specifically[24], the average flux was estimated to be 10.3–15.4 $g \cdot m^{-2} \cdot s^{-1}$ within 3 min of the holding time, 3.6 $g \cdot m^{-2} \cdot s^{-1}$ between 3–20 min and 0.1 between 20–40 min at 1650°C. Thus, the first 30 min of the process were modelled, keeping in mind that aluminothermic reduction was assumed to last for 20 min, followed by 10 min of additional time needed for the TBRC tapping. The objective was to determine the occurrence of slag solidification depending on the burner power and TBRC inclination angle. Regarding the last one, vertically oriented TBRC (θ = 90°, see Figure 2) can be modelled with a 2D axisymmetric model, and

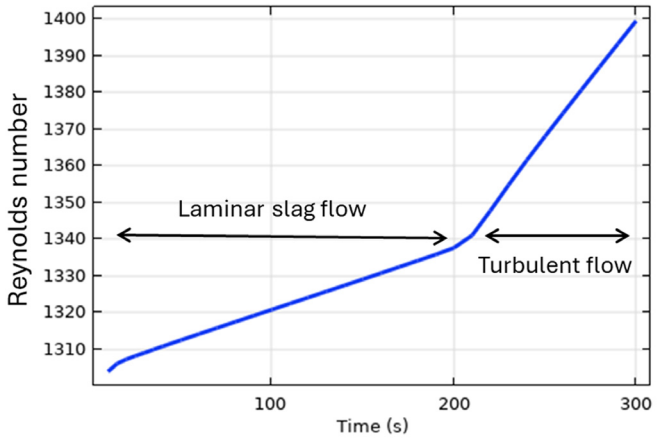

Figure 11. **Reynolds number for slag at 5 rpm and 600 kW burner power in a horizontal TBRC.**

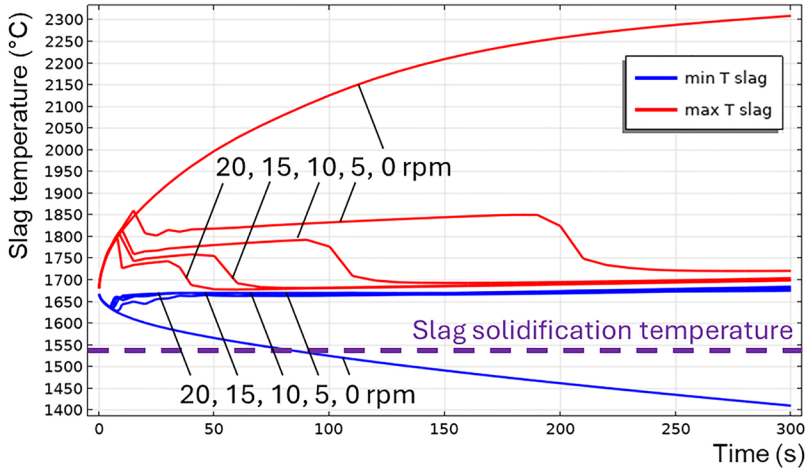

Figure 12. **Maximum and minimum slag temperature at different rotation frequencies and 600 kW burner power in a horizontal TBRC.**

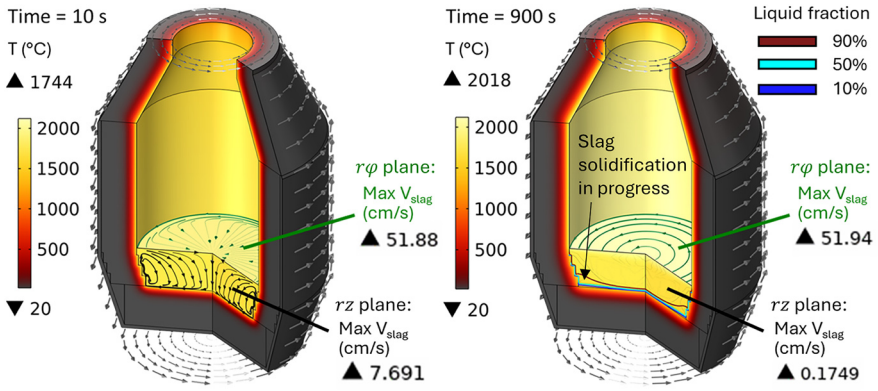

Figure 13. **Temperature field and slag velocity at 10 rpm and 600 kW burner power in a vertical TBRC.**

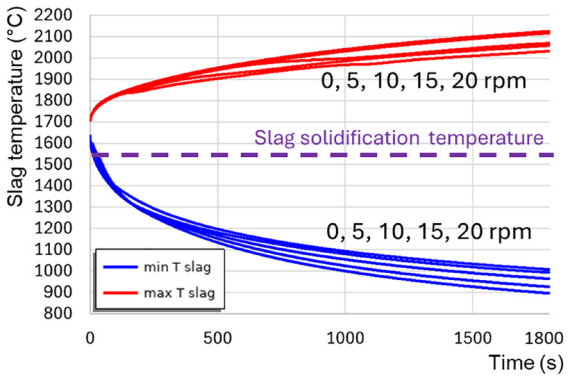

Figure 14. Maximum and minimum slag temperature at different rotation frequencies and 600 kW burner power in a vertical TBRC.

horizontally oriented TBRC ($\theta = 0°$) with a 2D plane model, whereas any other angle ($0° < \theta < 90°$) requires a full 3D model. To be efficient with respect to the computation time, 2D models are prioritized over 3D models. Therefore, interpolation of the major quantities of interest between $\theta = 0°$ and 90° is performed instead of 3D modelling. In addition, only one rotation frequency of 10 rpm, as recommended by MINTEK, was modelled here. The temperature and velocity fields in a horizontal TBRC are shown in Figure 15 for a 600 kW burner power. The corresponding time evolution of the maximum T_{max} and minimum T_{min} slag temperatures is shown in Figure 16. Initially, T_{min} drops to 850°C due to direct contact with the metal, whose initial temperature is 800°C. This causes slag solidification directly under the metal layer (see the liquid fraction isolines in Figure 15 at $t = 10$ s). During the next 200 s, owing to the reaction heat, T_{min} increased back to the initial slag temperature $T_{0,s} = 1670$°C (see Figure 16). At this point, the previously frozen slag is fully remelted without any risk to furnace operation. Further TBRC heating increases T_{max} at the metal-slag interface to 2280°C. At the same time, T_{min} in the middle of the larger laminar convective vortex (see $t = 600$ s in Figure 15) remains equal to $T_{0,s}$ owing to the poor mixing. At $t \approx 700$ s, see Figure 16, a transition to a turbulent flow regime occurs in the slag, resulting in a significant turbulent thermal conductivity that homogenizes the temperature across the slag layer and brings T_{min} and T_{max} closer. Further heating increased both T_{min} and T_{max} until the chemical reaction was complete at $t = 1200$ s. Subsequently, during $1200 \text{ s} < t < 1800$ s, the slag temperature was maintained at an almost constant value owing to the operating burner and turbulent mixing in the slag layer. Thus, there is no risk of slag solidification if the horizontally oriented TBRC operates at 10 rpm and 600 kW burner power.

Now, let us reduce the burner power. Figure 17 presents T_{min} and T_{max} in a horizontally oriented TBRC at 10 rpm and 164 kW burner power. This is the adjusted burner power that is sufficient to maintain the slag in a liquid state during the first 30 min of the process. A transition to a turbulent flow regime was not observed in this case. T_{max} increased up to 2150°C owing to the reaction heat and then dropped at 1200 s as the reaction stopped. T_{min} in the middle of the convective vortex remains equal to $T_{0,s}$ until $t = 1700$ s, and then starts to decrease owing to heat losses but does not reach the solidification temperature $T_{sol} = 1540$°C during the simulated times. Therefore, there was no risk of slag solidification in this furnace configuration.

Now, let us remove the burner and see if only the aluminothermic reduction power is sufficient to maintain the slag in a liquid state. The time evolution of slag temperature is shown in Figure 18. As one can see, the slag starts to solidify very quickly after the end of the reaction (see $t = 1500$ s in Figure 18). As before, the slag temperature in the middle of the convective vortex remained equal to the initial slag temperature $T_{0,s}$. In Figure 18 the mid-vortex temperature is represented by T_{min} for $500 \text{ s} < t < 1300$ s and by T_{max} for $t > 1500$ s. At $t = 1800$ s, slag solidification occurs primarily on the slag-metal and slag-refractory interfaces, resulting in the formation of a freeze-lining. Thus, there was a risk of slag solidification in this case.

Regarding the vertical TBRC orientation, as shown above, even with a maximum burner power of 600 kW, the slag solidifies at the bottom of the pool owing to inefficient stirring. Even the presence of additional heating at the metal-slag interface due to aluminothermic reduction is not sufficient to keep the slag in a liquid state, as shown in Figure 19. Note that the 0 rpm case is modelled here, as T_{min} and T_{max} are essentially independent

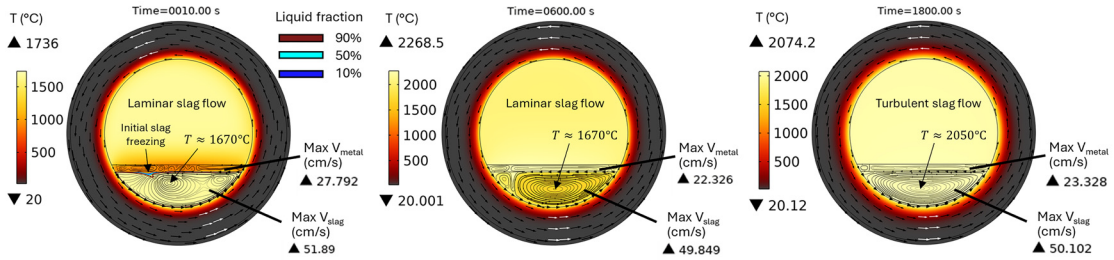

Figure 15. **Temperature and velocity fields at 10 rpm and 600 kW burner power in a horizontal TBRC.**

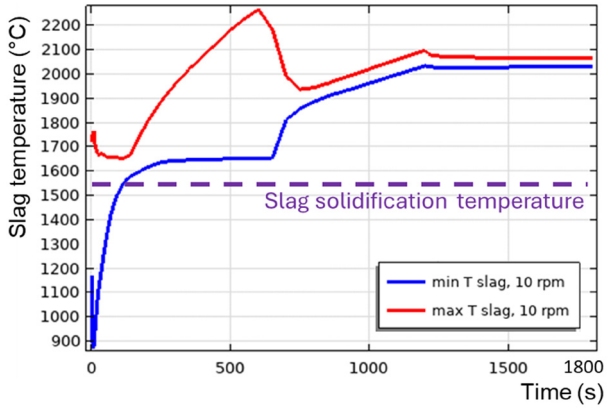

Figure 16. **Maximum and minimum slag temperature at 10 rpm and 600 kW burner power in a horizontal TBRC.**

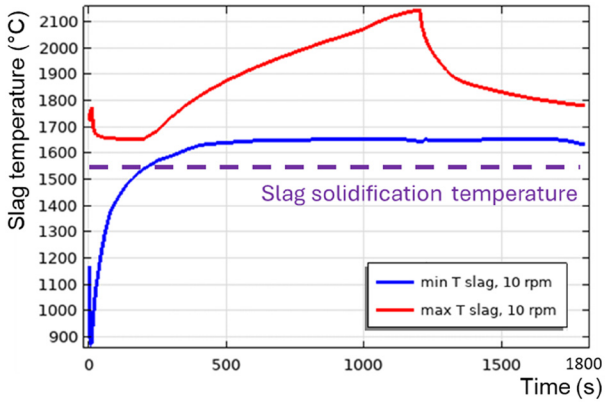

Figure 17. **Maximum and minimum slag temperature at 10 rpm and 164 kW burner power in a horizontal TBRC.**

of the rotation frequency in the vertical TBRC, as shown in Figure 14. The existence of the Rayleigh-Bénard instability in the metal layer and of the Rayleigh-Taylor instability in the slag is demonstrated in Figure 20.

All the above results are summarized in a 2D diagram of the occurrence of slag solidification depending on the burner power and TBRC inclination angle, as shown in Figure 21 (left). In this diagram, the location of the border between the red zone ("Risk of slag solidification") and green zone ("Slag remains liquid") is defined by condition $T_{min} = T_{sol}$, where T_{sol} = 1540°C is the slag solidification temperature, and T_{min} is the minimum

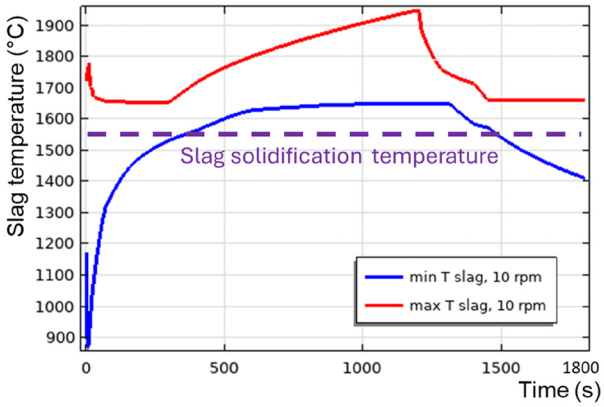

Figure 18. **Maximum and minimum slag temperature at 10 rpm and 0 kW burner power in a horizontal TBRC.**

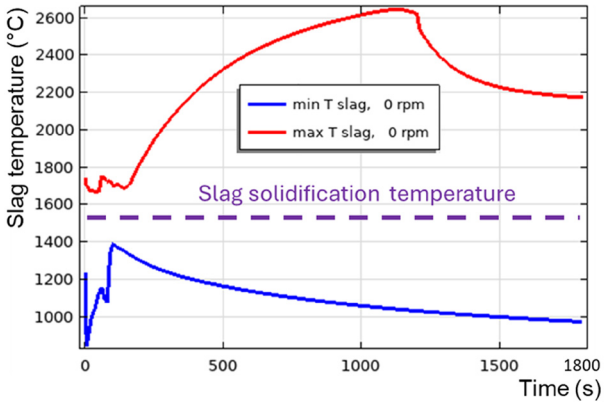

Figure 19. **Maximum and minimum slag temperature at 0 rpm and 600 kW burner power in a vertical TBRC.**

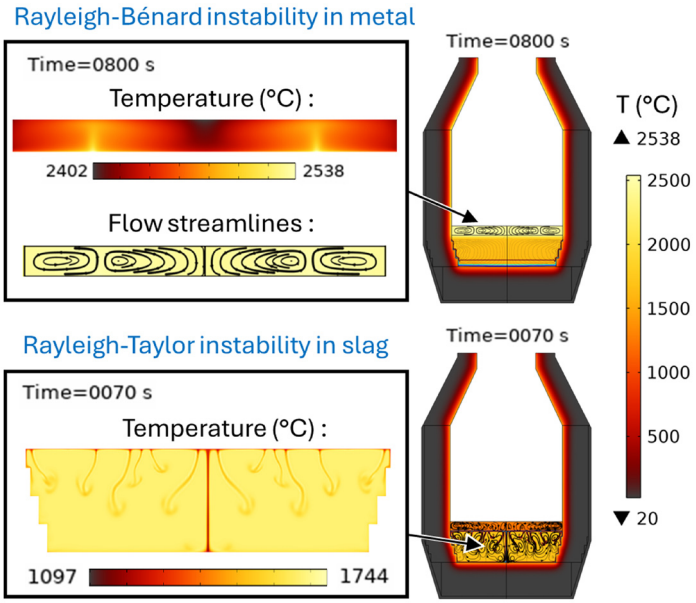

Figure 20. **Rayleigh-Bénard instability in the metal phase and Rayleigh-Taylor instability in the slag phase at 0 rpm and 600 kW burner power in a vertical TBRC.**

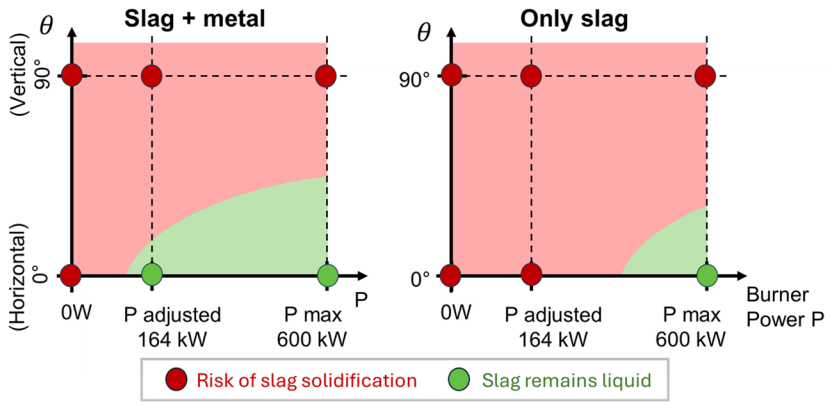

Figure 21. Occurrence of slag solidification depending on the burner power and on the TBRC inclination angle.

slag temperature at t = 1800 s obtained by interpolation between available diagram points. Finally, if the metal is not charged into the TBRC and only slag is present, the absence of heat from the aluminothermic reduction is compensated by the increase in the burner power, which shifts the above diagram to the right, as shown in Figure 21 (right).

The above-presented modelling approach and numerical findings suggest the following general takeaways that can inform decision-making and process improvements in similar TBRC operations:

- Reducing the TBRC inclination angle θ, so that its axis of rotation is getting closer to a horizontal orientation, improves the charge mixing and reduces the risk of slag solidification.
- In the limiting case of a horizontally oriented TBRC (θ = 0), slag solidification can be effectively avoided even at a rotation frequency as low as 1 rpm.
- The optimum burner power, specific to each TBRC design and refractory, can be determined through numerical modelling to prevent charge solidification.
- Once the optimum burner power is identified for a given charge composition, it can be adjusted for other compositions by accounting for the slag-metal reaction power, estimated from reaction energy and empirical reaction time.
- By increasing the charge temperature and the TBRC rotation frequency, a particular threshold Reynolds number can be reached, above which the flow transitions to a turbulent regime, which significantly improves the charge mixing and increases the rate of chemical reaction.

7. Conclusions

Numerical modelling of the top-blown rotary converter (TBRC) designed by MINTEK was presented. It is shown that the internal surface of TBRC can be preheated to 1650°C in less than 30 min if the useful burner power is 600 kW. Most of the thermal energy (81.2% in the steady state) is lost by thermal radiation from the inside of the TBRC towards the ambient environment through the opening at the top of the TBRC. Thus, the use of a furnace lid is strongly recommended to prevent significant heat loss. The occurrence of slag solidification depending on the burner power and TBRC orientation was assessed in 2D diagrams. The model of the charged TBRC shows that the horizontal TBRC orientation is the most favorable for charge stirring. As long as it rotates even at 1 rpm, stirring is efficient for maintaining the slag in a liquid state. In contrast, in vertically oriented TBRC, stirring is not efficient at any rotation frequency (tested up to 20 rpm) and leads to slag solidification at the bottom of the pool. Even a maximum burner power of 600 kW, together with the aluminothermic reduction heat, is not sufficient to avoid slag solidification in a vertical TBRC. However, an optimum burner power of 164 kW exists in the horizontal TBRC. This power, together with the reaction heat, is sufficient to maintain the slag in a liquid state during the first 30 min of the process, if the furnace is horizontally oriented. The modelling work resulted in the creation of a powerful decision-making tool that plays a

pivotal role in the comprehensive numerical support provided for the pilot campaign of the SisAl Pilot project. This tool permits exploration of new optimal configurations.

The broader-level findings can be summarized as follows. One can improve the charge mixing and reduce the risk of slag solidification by reducing the TBRC inclination angle θ and by imposing at least 1 rpm rotation frequency. The optimum burner power can be estimated based on a numerical simulation of a given TBRC design, combined with an empirical estimate of the chemical reaction power. At specific rotational speeds, a threshold Reynolds number can be exceeded, triggering a transition to turbulent flow that significantly enhances charge mixing and accelerates chemical reactions.

We acknowledge that experimental validation and comparison with established benchmarks would further strengthen our findings. We consider this to be an important direction for future work and encourage experimental studies to help validate our predictions.

Data and software availability

Repository: Zenodo. Dataset title: "Refractory materials used in the numerical model of TBRC".

https://doi.org/10.5281/zenodo.13880322[14]. This project contains the following underlying data:

Data file 1: "Insulation fibre 1260 ST-RB.png" (Data sheet for the properties of 1260 ST-RB insulation fibre)

Data file 2: "Refractory bricks VR 90B.png" (Data sheet for the properties of VR 90B refractory bricks)

Data file 3: "Castable refractory L-Cast 18.png" (Data sheet for the properties of L-Cast 18 castable refractory)

Data are available under the terms of the Creative Commons Attribution 4.0 International licence.

References

1. Darmana D, Olsen JE, Tang K, *et al.*: **Modelling concept for submerged arc furnaces.** In: *ninth international conference on CFD in the minerals and process industries CSIRO.* Melbourne, Australia, 2012; 10–12.
2. Abolpour B, Shamsoddini R: **Mechanism of reaction of silica and carbon for producing silicon carbide.** *Progress in Reaction Kinetics and Mechanism.* 2020; **45**: 1468678319891416. **Publisher Full Text**
3. Li F, Yang K, Fu W, *et al.*: **Carbothermal reduction of SiO_2 using different coal.** *Silicon.* 2024; **16**(5): 1967–1976. **Publisher Full Text**
4. Zhu M, Philipson H, Blandhol K, *et al.*: **Pilot-Scale Aluminothermic Production of Silicon Alloy and Alumina-Rich Slag.** *ACS Sustain Chem Eng.* 2024; **12**(40): 14795–14809. **PubMed Abstract** | **Publisher Full Text** | **Free Full Text**
5. Philipson H, Blandhol K, Engvoll K, *et al.*: **Preliminary techno-economic considerations of the SisAl process-closing materials loops through industrial symbiosis.** *Proceedings of the Silicon for the Chemical & Solar Industry XVI.* 2022. **Reference Source**
6. Khoei AR, Masters I, Gethin DT: **Numerical modelling of the rotary furnace in aluminium recycling processes.** *J Mater Process Technol.* 2003; **139**(1–3): 567–572. **Publisher Full Text**
7. Kolczyk E, Miczkowski Z, Czernecki J: **Numerical investigation of heat exchange in rotary furnace.** *Arch Metall Mater.* 2017; **62**(1): 149–153. **Publisher Full Text**
8. Reynolds QG, Erwee MW, Tsebe SP: **Toward computational models of metallurgical converting processes.** *Eleventh South African Conference on Computational and Applied Mechanics.* SACAM 2018, Vanderbijlpark, South Africa, 17-19 September 2018. **Reference Source**
9. El-Shiekh H, El-Fawakhry MK, Mitwally ME, *et al.*: **Production of reduced iron from mill scale waste using tilting rotary furnace.** *Results Mater.* 2023; **19**: 100429. **Publisher Full Text**
10. Odenthal HJ, Falkenreck U, Schlüter J: **CFD simulation of multiphase melt flows in steelmaking converters.** In: *ECCOMAS CFD 2006: Proceedings of the European Conference on Computational Fluid Dynamics, Egmond aan Zee, The Netherlands, September 5-8, 2006.* Delft University of Technology; European Community on Computational Methods in Applied Sciences (ECCOMAS). **Reference Source**
11. Crego O, Ferrín JL, Gómez D, *et al.*: **Transient mathematical modelling of a gas rotary furnace for melting slag.** *Appl Therm Eng.* 2024; **246**: 122928. **Publisher Full Text**
12. Jardy A: **Modélisation mathématique et simulation numérique de procédé de refusion à l'arc sous vide.** 2005.
13. Malhotra A, Kang SS: **Turbulent Prandtl number in circular pipes.** *Int J Heat Mass Transf.* 1984; **27**(11): 2158–2161. **Publisher Full Text**
14. Semenov S: **Refractory materials used in the numerical model of TBRC.** 2 October, 2024. **http://www.doi.org/10.5281/zenodo.13880322**
15. **NIST (Natioanl Institute of Standards and Technology) chemistry WebBook**. **Reference Source**
16. Leitner M, Leitner T, Schmon A, *et al.*: **Thermophysical properties of liquid aluminum.** *Metall Mater Trans A.* 2017; **48**(6): 3036–3045. **Publisher Full Text**
17. Assael MJ, Armyra IJ, Brillo J, *et al.*: **Reference data for the density and viscosity of liquid cadmium, cobalt, gallium, indium, mercury, silicon, thallium, and zinc.** *J Phys Chem Ref Data.* 2012; **41**(3): 033101. **Publisher Full Text**
18. Bohdansky J, Schins HEJ: **Surface tension and density of the liquid earth alkaline metals Mg, Ca, Sr, Ba.** *J Inorg Nucl Chem.* 1968; **30**(9): 2331–2337. **Publisher Full Text**
19. Xin J, Gan L, Jiao L, *et al.*: **Accurate density calculation for**

molten slags in SiO_2-Al_2O_3-CaO-MgO systems. *ISIJ International.* 2017; **57**(8): 1340–1349.
Publisher Full Text

20. Tang K, Gouttebroze S, Ma X, *et al.*: **Representation of the multiphysical properties of SiO_2-Al_2O_3-CaO slags by deep neural networks.** In: *Proceedings of the 16th International Ferro-Alloys Congress (INFACON XVI).* (virtual), 2021.
Publisher Full Text

21. Tang K, van der Eijk C, Gouttebroze S, *et al.*: **Rheological properties of Al_2O_3--CaO--SiO_2 slags.** *Calphad.* 2022; **77**: 102421.
Publisher Full Text

22. Dinsdale AT, Quested PN: **The viscosity of aluminium and its alloys--A review of data and models.** *J Mater Sci.* 2004; **39**: 7221–7228.
Publisher Full Text

23. Mills KC, Yuan L, Jones RT: **Estimating the physical properties of slags.** *J S Afr Inst Min Metall.* 2011; **111**(10): 649–658.
Reference Source

24. Philipson HG, Wallin M, Einarsrud KE: **Investigation of Liquid–Liquid Reaction Phenomena of Aluminum in Calcium Silicate Slag.** *Materials (Basel).* 2024; **17**(7): 1466.
PubMed Abstract | **Publisher Full Text** | **Free Full Text**

Open Peer Review

Current Peer Review Status: ✔ ✔ ✘ ✔

Version 2

Reviewer Report 02 September 2025

https://doi.org/10.21956/openreseurope.22542.r57528

© **2025 Coetsee T.** This is an open access peer review report distributed under the terms of the Creative Commons Attribution License, which permits unrestricted use, distribution, and reproduction in any medium, provided the original work is properly cited.

✔ **Theresa Coetsee**
University of Pretoria, Pretoria, Gauteng, South Africa

The article describes the development of a CFD model of the heat transfer in a pilot plant rotary converter heated by a 600kW oxy-fuel burner. The main aim of the model is to serve as a plant design tool for construction and to direct process operational issues to be addressed during plant engineering design. In these aims, the model is successful.

Literature: Add the following similar paper for completeness: [Reference 1]

Sufficient details: Some slag-metal properties are derived from an artificial neural network-based tool based on FactSage data, which is not accessible to all. However, others can approximate these properties as well.

Technical questions:
1. The brick surface exceeds the refractory melting point in Figure 5, so the burner energy needs to be scaled back. Mention this.

2. According to section 4.3 , the method used to input the burner energy is simplified as a boundary condition. The CFD modelling of burner characteristics is quite complex and the flame profile and density influence the flame radiation efficiency. None of these effects are present in the current model. To better gauge the heat balance components in this model and future refinements, it is instructive to express heat transfer values in kW/m^2 over each surface, not only as kW as in Figure 6. A simple table with square meter areas and kW and resultant kW/m^2 for the steady-state conditions will be sufficient. In this way the design numbers can be compared to other models and the plant design can be easily scaled.

Although this is not a validated detailed model, it serves its purpose as stated in the introduction. Future validation against operational data will be interesting.

References

1. Zhang Y, Barr P, Ray Meadowcroft T: Continuous scrap melting in a short rotary furnace.

Minerals Engineering. 2008; **21** (2): 178-189 Publisher Full Text

Is the work clearly and accurately presented and does it cite the current literature?
Partly

Is the study design appropriate and does the work have academic merit?
Yes

Are sufficient details of methods and analysis provided to allow replication by others?
Partly

If applicable, is the statistical analysis and its interpretation appropriate?
Not applicable

Are all the source data underlying the results available to ensure full reproducibility?
Partly

Are the conclusions drawn adequately supported by the results?
Yes

Competing Interests: No competing interests were disclosed.

Reviewer Expertise: Pyrometallurgy, process design.

I confirm that I have read this submission and believe that I have an appropriate level of expertise to confirm that it is of an acceptable scientific standard.

Reviewer Report 29 August 2025

https://doi.org/10.21956/openreseurope.22542.r56468

© 2025 Donato L. This is an open access peer review report distributed under the terms of the Creative Commons Attribution License, which permits unrestricted use, distribution, and reproduction in any medium, provided the original work is properly cited.

Laura Donato
Universite Libre de Bruxelles, Brussels, Brussels, Belgium

The authors have improved the manuscript in this revised version. The comments and suggestions from the previous review round have been carefully addressed, and the paper is now clear, well-structured, and scientifically sound. The methodology is appropriate and well-explained, the results are coherent and well-presented, and the conclusions are supported by the findings.
I have no further major concerns. I recommend **acceptance** of this version for publication.

Competing Interests: No competing interests were disclosed.

Reviewer Expertise: Modelling Combustion systems, Machine Learning, Chemical Engineering

I confirm that I have read this submission and believe that I have an appropriate level of expertise to confirm that it is of an acceptable scientific standard.

Reviewer Report 20 August 2025

https://doi.org/10.21956/openreseurope.22542.r56469

© 2025 Bhoi N. This is an open access peer review report distributed under the terms of the Creative Commons Attribution License, which permits unrestricted use, distribution, and reproduction in any medium, provided the original work is properly cited.

Neeraj Kumar Bhoi
Mechatronics Engineering, Banasthali University (Ringgold ID: 29803), Jaipur, Rajasthan, India

Accept

Competing Interests: No competing interests were disclosed.

Reviewer Expertise: Sustainable manufacturing and finite element modeling study.

I confirm that I have read this submission and believe that I have an appropriate level of expertise to confirm that it is of an acceptable scientific standard.

Version 1

Reviewer Report 23 January 2025

https://doi.org/10.21956/openreseurope.20114.r49082

© 2025 Kuang S. This is an open access peer review report distributed under the terms of the Creative Commons Attribution License, which permits unrestricted use, distribution, and reproduction in any medium, provided the original work is properly cited.

Shibo Kuang
Monash University, Clayton, Victoria, Australia

This manuscript presents a numerical study of a top-blown rotary converter under specific conditions. However, the paper is poorly presented, and the results are unconvincing. Several major issues are outlined below:

1. The numerical model is not adequately justified, and key details are missing. It is unclear whether the interfaces among gas, metal, and slag were modeled, and, if so, how this was achieved. Additionally, the coupling between flows and heat transfer, as well as the

interactions among different phases, are not clearly explained. Furthermore, the approach used for modeling solidification is entirely omitted, leaving significant methodological gaps.
2. The model has not been validated, which undermines the credibility of the results. Without validation against experimental data or established benchmarks, the reliability and accuracy of the study cannot be assessed.
3. The practical applicability of the results is unclear. The manuscript does not explain how the findings could be used to solve problems or improve the operation of top-blown rotary converters, making their relevance questionable.
4. The study fails to provide adequate context regarding progress in the field. Existing research gaps are not clearly identified, and the contribution of this work to advancing the field is not demonstrated.
5. The analysis presented in the study lacks depth. Key findings are not explored in detail, and important insights are either overlooked or insufficiently addressed.
6. The conclusions are overly specific and do not offer broader insights or generalizations. They should be expanded to highlight the implications of the findings and their relevance to the wider research community.

Is the work clearly and accurately presented and does it cite the current literature?
No

Is the study design appropriate and does the work have academic merit?
No

Are sufficient details of methods and analysis provided to allow replication by others?
No

If applicable, is the statistical analysis and its interpretation appropriate?
No

Are all the source data underlying the results available to ensure full reproducibility?
No source data required

Are the conclusions drawn adequately supported by the results?
No

Competing Interests: No competing interests were disclosed.

Reviewer Expertise: Computational process engineering

I confirm that I have read this submission and believe that I have an appropriate level of expertise to state that I do not consider it to be of an acceptable scientific standard, for reasons outlined above.

Author Response 30 Jun 2025

Sergey Semenov

We are grateful to the reviewer for the useful and insightful comments, which helped us to improve key aspects of our research article. Our responses to the individual comments in the report are provided below.

1. The numerical model is not adequately justified, and key details are missing. It is unclear whether the interfaces among gas, metal, and slag were modeled, and, if so, how this was achieved. Additionally, the coupling between flows and heat transfer, as well as the interactions among different phases, are not clearly explained. Furthermore, the approach used for modeling solidification is entirely omitted, leaving significant methodological gaps.

Authors: We appreciate the reviewer's feedback and would like to clarify the aspects raised regarding the justification and details of our numerical model. The boundary conditions, formulated as mathematical equations, define the exchange of momentum and energy at the interfaces and fully describe our approach to modeling the interfaces among gas, metal, and slag. These equations are explicitly presented in Section 4. To further enhance clarity, we have added additional explanations in Section 4 to explicitly outline how these interfaces are treated in our model. In particular: "The interfaces among gas, metal and slag are assumed to be fixed in space. The free surface displacement is disregarded, since the stratification of the phases in the Earth's gravitational field is assumed to prevent significant interfaces displacement." The coupling between flow and heat transfer is explicitly addressed by incorporating the influence of both flow velocity and turbulent thermal conductivity on the heat transfer process. Specifically, convective heat transfer is driven by the fluid motion, with velocity fields influencing temperature distribution. Additionally, the turbulence model accounts for enhanced thermal transport by incorporating turbulent thermal conductivity, which plays a key role in energy exchange within the system. These aspects are carefully described in Section 4.3, providing a comprehensive explanation of the coupling mechanisms implemented in the model. Additionally, the properties of metal and slag, including density and dynamic viscosity, are treated as functions of temperature, creating a strong bidirectional coupling between flow and heat transfer. These aspects of the model are clarified in sections 4 and 5 of the revised article. Regarding the modeling of solidification, our approach is explicitly described at the beginning of Section 4.3. Specifically, we employ the Apparent Heat Capacity method. This methodology effectively captures the phase transition process and is consistent with established modeling approaches in the field. We hope these clarifications address the reviewer's concerns and demonstrate the completeness of our numerical model. We remain open to providing further elaboration if needed.

2. The model has not been validated, which undermines the credibility of the results. Without validation against experimental data or established benchmarks, the reliability and accuracy of the study cannot be assessed.

Authors: We appreciate the reviewer's concern about model validation. We acknowledge that experimental validation is a crucial step in establishing the accuracy of modelling approaches. However, experimental validation was beyond the scope of the current project. The primary objective of this study was to develop and explore a computational framework to numerically validate the new TBRC design and to gain insight into its optimal operation prior to its construction. This assumes the non-existence of the equipment and the absence

of experimental data during the modelling work. A posteriori, when the new equipment was built, it was not possible to collect sufficient experimental data for the model validation, because the real operating conditions were not the same as in the model (for example, the TBRC lid was used in real operating conditions, as is recommended in this article). We acknowledge that experimental validation or comparison with established benchmarks would further strengthen our findings. We consider this to be an important direction for future work and encourage experimental studies to help validate our predictions (the appropriate statement is added to the conclusions).

3. The practical applicability of the results is unclear. The manuscript does not explain how the findings could be used to solve problems or improve the operation of top-blown rotary converters, making their relevance questionable.

Authors: We would like to clarify that the study was carried out with a focus on a specific experimental Top-Blown Rotary Converter (TBRC) unit being designed and constructed at Mintek (South Africa). The objective was to analyze and optimize certain operational aspects - such as burner power, rotation frequency and inclination angle - within the context of that unit. While the scope of the study was limited to this particular TBRC, the methodology and findings offer broader insights that can be adapted to similar converter systems. For example, the modeling approach can be used by engineers to assess and enhance the performance of their own converters, especially under comparable conditions. To address this more clearly, we have revised the manuscript to include a discussion of how the results can inform decision-making and process improvements in other TBRC operations (see the end of section 6).

4. The study fails to provide adequate context regarding progress in the field. Existing research gaps are not clearly identified, and the contribution of this work to advancing the field is not demonstrated.

Authors: We appreciate the reviewer’s comment and understand the importance of clearly situating the study within the broader context of the field. In this work, our focus was on addressing a specific engineering challenge within the SisAl Pilot project, rather than providing a comprehensive review of the field. Nevertheless, we have revised the introduction to better highlight relevant prior work, clarify existing research gaps, and more explicitly articulate the contribution of our study within this targeted context.

5. The analysis presented in the study lacks depth. Key findings are not explored in detail, and important insights are either overlooked or insufficiently addressed.

Authors: We thank the reviewer for their thoughtful comment. While we agree that a more in-depth analysis could provide additional insights, we respectfully note that the primary objective of this numerical study is to validate a specific TBRC design by verifying its key operational aspects through simulations prior to construction, thereby ensuring successful commissioning and reliable operation thereafter. While further in-depth analysis of the findings is possible, it is not required for the purposes of the SisAl project and is therefore beyond the scope of this study. In the revised manuscript we have listed key findings at the end of section 6.

6. The conclusions are overly specific and do not offer broader insights or generalizations. They should be expanded to highlight the implications of the findings and their relevance to the wider research community.

Authors: We thank the reviewer for their helpful comment. In the revised manuscript, the broader-level findings are listed at the end of section 6 and are also summarized in the conclusions. We hope that this modification addresses the concerns of the reviewer.

Competing Interests: No competing interests were disclosed.

Reviewer Report 10 January 2025

https://doi.org/10.21956/openreseurope.20114.r46861

© 2025 Donato L. This is an open access peer review report distributed under the terms of the Creative Commons Attribution License, which permits unrestricted use, distribution, and reproduction in any medium, provided the original work is properly cited.

?

Laura Donato
Universite Libre de Bruxelles, Brussels, Brussels, Belgium

This study evaluates the aluminothermic reduction of silica in a top-blown rotary converter (TBRC) heated by an oxy-fuel burner, offering low CO_2 emissions compared to carbothermic methods. Modeling focuses on the TBRC's thermal performance, assessing slag solidification risks, optimal burner power, and the effects of inclination and rotation of the TBRC. The software used for this purpose is COMSOL Multiphysics.

Strengths:
The research supports sustainable silicon production by promoting carbon-efficient technologies, in line with environmental goals. I found the paper interesting and consider it a strong starting point for sustainable silicon production. The geometry of the TBRC is well-defined, and the clarity of the methodology is evident throughout the work. Many of the figures are well-crafted and meaningful. However, I would have appreciated including a real-life image of the TBRC to enhance the understanding of the setup further. Overall, the paper provides valuable insights and a clear contribution to the field.

Drawbacks:
To improve this study, I propose the following:
- Literature Review: a more in-depth literature review on this type of research is necessary. The study does not reference similar works or discussions on this topic. Highlighting differences and strengths compared to existing studies would provide valuable outcomes and enhance the impact of the work, especially in the sustainability scenario.
- Chemical Reactions: Including the chemistry behind aluminothermic reduction and discussing its comparison with carbothermic would enrich the study. A detailed explanation of the processes

could also help underline the significance of the proposed approach.
- Experimental Data: Adding experimental data would significantly strengthen the study's relevance and application, though I understand it may be challenging to incorporate at this stage.

Additional comments:
- Was the computational mesh developed symmetrically? Do the 27,600 finite elements represent only half of the entire TBRC?
- Could Figure 12 be made more comprehensive? I believe the labeling could be improved for better clarity.
- Section 6.3: Why was the aluminothermic reduction assumed to last 20 minutes? Is there a reference or experimental data that justifies this duration?

Is the work clearly and accurately presented and does it cite the current literature?
Partly

Is the study design appropriate and does the work have academic merit?
Partly

Are sufficient details of methods and analysis provided to allow replication by others?
Partly

If applicable, is the statistical analysis and its interpretation appropriate?
Partly

Are all the source data underlying the results available to ensure full reproducibility?
Partly

Are the conclusions drawn adequately supported by the results?
Partly

Competing Interests: No competing interests were disclosed.

Reviewer Expertise: Modelling Combustion systems, Machine Learning, Chemical Engineering

I confirm that I have read this submission and believe that I have an appropriate level of expertise to confirm that it is of an acceptable scientific standard, however I have significant reservations, as outlined above.

Author Response 30 Jun 2025

Sergey Semenov

We are grateful to the reviewer for the useful and insightful comments, which helped us to improve key aspects of our research article. Our responses to the individual comments in the report are provided below.

- Literature Review: a more in-depth literature review on this type of research is necessary.

The study does not reference similar works or discussions on this topic. Highlighting differences and strengths compared to existing studies would provide valuable outcomes and enhance the impact of the work, especially in the sustainability scenario.

Authors: Thank you for your valuable feedback. Additional literature sources on the sustainability and economic viability of the SisAl process, as well as on numerical modelling of rotary furnaces are cited and shortly discussed in the article introduction. Description of differences in thermal boundary conditions compared to a recent literature source is mentioned in section 4.3. Another key distinguishing aspect of our work compared to previous studies is the problem geometry and operating conditions, which directly influence the flow dynamics and heat transfer.

- Chemical Reactions: Including the chemistry behind aluminothermic reduction and discussing its comparison with carbothermic would enrich the study. A detailed explanation of the processes could also help underline the significance of the proposed approach.

Authors: The revised article introduction describes the chemical reactions of the traditional carbothermic reduction of silica and the aluminothermic reduction proposed in the SisAl Pilot project. The advantages of the SisAl process over the carbothermic process are explained in detail, justifying its significance and economic viability.

- Experimental Data: Adding experimental data would significantly strengthen the study's relevance and application, though I understand it may be challenging to incorporate at this stage.

Authors: We appreciate the reviewer's insightful comment on the need for experimental validation to support our numerical results. However, experimental validation was beyond the scope of this study. The whole purpose of this work is to numerically validate the new TBRC design and to gain insight into its optimal operation prior to its construction. This assumes the non-existence of the equipment and the absence of experimental data during the modelling work. A posteriori, when the new equipment was built, it was not possible to collect sufficient experimental data for the model validation, because the real operating conditions were not the same as in the model (for example, the TBRC lid was used in real operating conditions, as is recommended in this article). We acknowledge that experimental validation or comparison with established benchmarks would further strengthen our findings. We consider this to be an important direction for future work and encourage experimental studies to help validate our predictions (the appropriate statement is added to the conclusions).

Additional comments:
- Was the computational mesh developed symmetrically? Do the 27,600 finite elements represent only half of the entire TBRC?

Authors: Since the computation is done in a 2D axisymmetric geometry, the computational domain (see Figure 3) represents only half of the entire TBRC in the r-z plane. The other half of TBRC does not exist in a 2D axisymmetric formulation and therefore cannot be meshed. Thus, we can say that 27600 finite elements represent only half of the entire TBRC.

- Could Figure 12 be made more comprehensive? I believe the labeling could be improved for better clarity.

Authors: Thank you for this suggestion. The labeling of Figure 12 is improved in the revised article.

- Section 6.3: Why was the aluminothermic reduction assumed to last 20 minutes? Is there a reference or experimental data that justifies this duration?

Authors: We appreciate the reviewer's valuable comment on the need for justification, which helps us to improve the quality of our work. The aluminothermic reduction is assumed to last for 20 minutes based on experimental investigations carried out in the framework of the SisAl Pilot project. A detailed explanation with a literature source is given at the beginning of section 6.3 of the revised article.

Competing Interests: No competing interests were disclosed.

Reviewer Report 28 November 2024

https://doi.org/10.21956/openreseurope.20114.r46858

© 2024 Bhoi N. This is an open access peer review report distributed under the terms of the Creative Commons Attribution License, which permits unrestricted use, distribution, and reproduction in any medium, provided the original work is properly cited.

?

Neeraj Kumar Bhoi
Mechatronics Engineering, Banasthali University (Ringgold ID: 29803), Jaipur, Rajasthan, India

Strengths:

1. The study provides a comprehensive numerical model for analyzing preheating and charge heating in a top-blown rotary converter (TBRC) using COMSOL Multiphysics.
2. The use of the finite element method and detailed thermal and fluid dynamics modeling ensures accuracy and relevance.
3. The research contributes to sustainable silicon production by addressing carbon-emission-friendly technologies, aligning with global environmental priorities.
4. Clear presentation of results, including the influence of burner power, TBRC inclination angle, and rotation frequency, with practical recommendations to improve operational efficiency.
5. The creation of a decision-making tool adds value for real-world applications and pilot projects.

Areas for Improvement:

1. **Experimental Validation:** The paper relies entirely on numerical modeling. Incorporating experimental validation of the model's predictions would enhance credibility and applicability to real-world scenarios.

2. **Data Uncertainty:** Addressing uncertainties in material properties, boundary conditions, and numerical methods could improve reliability. Sensitivity analysis of key parameters would add depth.
3. **Generalization of Results:** The study focuses on specific configurations and conditions. Broadening the scope to include different TBRC designs and operational scenarios could increase its relevance.
4. **Economic Viability:** While the paper addresses technical aspects, incorporating a discussion on the economic feasibility of the proposed configurations would strengthen its industrial impact.
5. **Environmental Assessment:** A more detailed assessment of the environmental benefits, such as a reduction in CO2 emissions compared to traditional methods, would align better with sustainability goals.
6. **Visualization:** Some figures (e.g., temperature fields and slag behavior) could benefit from clearer annotations and labels to aid interpretation.
7. **Policy Implications:** Linking the findings to broader industrial standards or regulatory frameworks could highlight the significance of the work for policymakers.
8. **References to Prior Work:** The paper could discuss how this work builds on or differs from existing studies on TBRC and aluminothermic reduction, particularly addressing gaps in previous literature.

Is the work clearly and accurately presented and does it cite the current literature?
Partly

Is the study design appropriate and does the work have academic merit?
Partly

Are sufficient details of methods and analysis provided to allow replication by others?
Partly

If applicable, is the statistical analysis and its interpretation appropriate?
Partly

Are all the source data underlying the results available to ensure full reproducibility?
Partly

Are the conclusions drawn adequately supported by the results?
No

Competing Interests: No competing interests were disclosed.

Reviewer Expertise: Sustainable manufacturing and finite element modeling study.

I confirm that I have read this submission and believe that I have an appropriate level of expertise to confirm that it is of an acceptable scientific standard, however I have significant reservations, as outlined above.

Author Response 27 Jun 2025

Sergey Semenov

We are grateful to the reviewer for the useful and insightful comments, which helped us to improve key aspects of our research article. Our responses to the individual comments in the report are provided below.

1. Experimental Validation: The paper relies entirely on numerical modeling. Incorporating experimental validation of the model's predictions would enhance credibility and applicability to real-world scenarios.
Authors: We appreciate the reviewer's insightful comment on the need for experimental validation to support our numerical results. However, experimental validation was beyond the scope of this study. The whole purpose of this work is to numerically validate the new TBRC design and to gain insight into its optimal operation prior to its construction. This assumes the non-existence of the equipment and the absence of experimental data during the modelling work. A posteriori, when the new equipment was built, it was not possible to collect sufficient experimental data for the model validation, because the real operating conditions were not the same as in the model (for example, the TBRC lid was used in real operating conditions, as is recommended in this article). We acknowledge that experimental validation or comparison with established benchmarks would further strengthen our findings. We consider this to be an important direction for future work and encourage experimental studies to help validate our predictions (the appropriate statement is added to the conclusions).

2. Data Uncertainty: Addressing uncertainties in material properties, boundary conditions, and numerical methods could improve reliability. Sensitivity analysis of key parameters would add depth.
Authors: We appreciate the reviewer's valuable suggestion regarding the inclusion of additional parameters in the parametric study. We fully acknowledge the importance of exploring the sensitivity to material properties, numerical methods, and boundary conditions; however, extending the study to incorporate these factors would significantly increase the computational cost. Our current analysis already involves a parametric study on three key parameters (burner power, inclination angle and rotation frequency), leading to a three-dimensional parameter space. Introducing additional parameters would exponentially increase the number of simulations required, making the problem computationally prohibitive within the available resources. The numerical methods and boundary conditions used in this work are consistent with established best practice for modelling rotary converters, see for example [Crego et al. Transient mathematical modelling of a gas rotary furnace for melting slag. Applied Thermal Engineering. 2024;246:122928].

3. Generalization of Results: The study focuses on specific configurations and conditions. Broadening the scope to include different TBRC designs and operational scenarios could increase its relevance.
Authors: We appreciate the reviewer's suggestion regarding the broadening of the study to encompass additional designs and operational scenarios. We fully acknowledge that a more extensive exploration would enhance the general applicability of our findings. However, our study aims to provide an in-depth analysis of a well-defined configuration that is

representative of practical applications. Expanding the scope significantly would require a substantial increase in computational resources and analysis time, which is beyond the scope of current study. To ensure the robustness of our conclusions, we have selected the studied configuration based on its practical relevance and have conducted parametric studies to capture key trends. We believe that the insights gained from this work can serve as a foundation for future studies that may explore broader design variations and operating conditions. We hope this clarification addresses the reviewer's concern.

4. Economic Viability: While the paper addresses technical aspects, incorporating a discussion on the economic feasibility of the proposed configurations would strengthen its industrial impact.
Authors: We fully acknowledge that assessing economic viability is crucial for industrial applications. However, this study is primarily focused on the technical and physical aspects of the proposed configurations, with an emphasis on performance evaluation. Evaluating the economic feasibility for the specific configuration of the metallurgical reactor studied in this article is challenging, as the technology implemented in the studied process differs from the originally planned approach. For example, to mitigate the impact of load shedding in South Africa, electrical heating was replaced with a gas burner. It is important to note that this research is part of a larger collaborative effort involving multiple partners, and the economic feasibility of the overall SisAl process is assessed at a broader level. See for example the following reference [H. Philipson et al., Preliminary techno-economic considerations of the SisAl process-closing materials loops through industrial symbiosis. *Proceedings of the Silicon for the Chemical & Solar Industry XVI*], which is cited in the revised version of the article.

5. Environmental Assessment: A more detailed assessment of the environmental benefits, such as a reduction in CO2 emissions compared to traditional methods, would align better with sustainability goals.
Authors: As previously mentioned, the use of a gas burner is a mitigation measure that alters the CO_2 impact. The originally planned technology, which relied on electrical heating and aluminothermic reduction, would have resulted in nearly zero CO_2 emissions, except for those associated with electricity production. In this context, evaluating the environmental impact of a specific technological step that includes mitigation measures is not considered relevant.

6. Visualization: Some figures (e.g., temperature fields and slag behavior) could benefit from clearer annotations and labels to aid interpretation.
Authors: Figures 4, 7, 8, 12, 13, 15 are modified. Additional labels are added for temperature values and slag behavior.

7. Policy Implications: Linking the findings to broader industrial standards or regulatory frameworks could highlight the significance of the work for policymakers.
Authors: We fully acknowledge that aligning research with established guidelines enhances its impact, particularly for policymakers and industry stakeholders. The primary focus of this study has been on the technical and scientific aspects of the process, and an in-depth regulatory analysis was beyond its intended scope. Future work could explore this aspect in greater detail.

8. References to Prior Work: The paper could discuss how this work builds on or differs from existing studies on TBRC and aluminothermic reduction, particularly addressing gaps in previous literature.
Authors: Additional literature sources on the sustainability and economic viability of the SisAl process, as well as on numerical modelling of rotary furnaces are cited and shortly discussed in the article introduction. Description of differences in thermal boundary conditions compared to a recent literature source is mentioned in section 4.3. Another key distinguishing aspect of our work compared to previous studies is the problem geometry and operating conditions, which directly influence the flow dynamics and heat transfer. We have now clarified this point in the introduction of the revised article.

Competing Interests: No competing interests were disclosed.